DEVELOPMENT OF A THREE-COMPONENT DOPPLER GLOBAL VELOCIMETRY SYSTEM

Graham S. Hawkes (*)
Dept. of Engineering Science
University of Oxford, UK
graham.hawkes@eng.ox.ac.uk

Dr. Steven. J. Thorpe (**)
Dept. of Aeronautical and
Automotive Engineering
Loughborough University, UK

Prof. Roger. W. Ainsworth
Dept. of Engineering Science
University of Oxford, UK

ABSTRACT

This paper describes the design and construction of a Three-Component Doppler Global Velocimetry System, primarily designed for capturing the instantaneous three-dimensional velocity field within a plane formed by a collimated laser sheet. Three-Component Doppler Global Velocimetry (3C-DGV) has several advantages over other planar techniques, for example Particle Image Velocimetry (PIV), namely that the resolution is typically at least an order of magnitude higher, only a single laser pulse is required to obtain the velocity field and that laser planes can be arranged perpendicular to major flow components.

NOMENCLATURE

F	Optics F-number
f_D	Doppler Shift
$\mathbf{f}$	Doppler Shifts Vector
f_L	Fourier Limited Linewidth
$\mathbf{G}$	Transform Matrix
M	Magnification
N_e	Number of electrons
$\mathbf{o_i}$	*i*th Observation Vector
$\mathbf{l}$	Laser Illumination Vector
$\mathbf{s}$	Sensitivity Vector
s_{ij}	Senstivity Coefficient
SNR	Signal to Noise Ratio
t_p	Pulse Duration (FWHM)
u_x	x-axis Velocity
u_y	y-axis Velocity
u_z	z-axis Velocity
$\mathbf{v}$	Velocity Vector
Δx	Pixel Dimension
λ_o	Laser Wavelength

1 - INTRODUCTION

The ultimate aim of an aerodynamicist is to numerically solve the Navier-Stokes equations for unsteady turbulent flows. For aerospace flows with high Reynolds numbers the number of grid points required to resolve the flow structures exceeds the capability of traditional Computational Fluid Dynamics (CFD) (**Lawson, 2004)**. This problem is solved by the use of flow modeling to limit the number of grid points to that obtainable with modern computers. Before any designer can use the software for design the models must be verified experimentally. Verification of the flow models requires experimental determination of the pressure, temperature and velocity fields within the geometry. This paper is concerned with the measurement of velocity (Velocimetry).

Traditional velocimetry uses probe techniques such as pitot tubes, hotwire anemometry or wedge probes. However, the presence of the probe distorts the local velocity field and the measurement is conducted at a single point. The pointwise nature of these techniques means that, for short duration test facilities, the velocity fields must be mapped using a large number of repeated experiments or of high speed traverses.

In order to minimize the invasive nature of measurement laser techniques were developed starting with Laser Doppler Velocimetry (LDV). However, LDV is a pointwise technique and a great deal of time is required to map a large velocity field. In order to reduce mapping times wholefield or 'global' techniques were developed, the most established of which being PIV.

Doppler Global Velocimetry (DGV) was first described by **Komine and Brosnan (1991)**. The technique has considerable advantages over PIV namely that the measurement resolution is higher, only a single laser pulse is required to obtain the velocity field and that laser planes can be arranged perpendicular to major flow components.

2 - THE DGV PRINCIPLE

DGV is often referred to as Planar Doppler Velocimetry (PDV), which reflects the planar nature of the technique. Both terms are widely used but the technique shall be referred to as DGV in this paper.

 * Email for correspondence ** Formerly at University of Oxford

DGV relies on the measurement of the frequency shift of radiation perceived by an observer as radiation is scattered from a moving object. The frequency shift is termed the *Doppler Shift* (f_D) and is dependent on the directions of the incident radiation, observation and the object velocity. The shift can be expressed in vectorial form as (see **Fig 1**),

$$f_D = \frac{\left(\hat{\mathbf{o}} - \hat{\mathbf{i}}\right)\cdot \mathbf{v}}{\lambda_o} \qquad (2.1)$$

Where,

$$\mathbf{v} = u_x\hat{\mathbf{i}} + u_y\hat{\mathbf{j}} + u_z\hat{\mathbf{k}} \qquad (2.2)$$

$$\mathbf{s} = \left(\hat{\mathbf{o}} - \hat{\mathbf{i}}\right) \qquad (2.3)$$

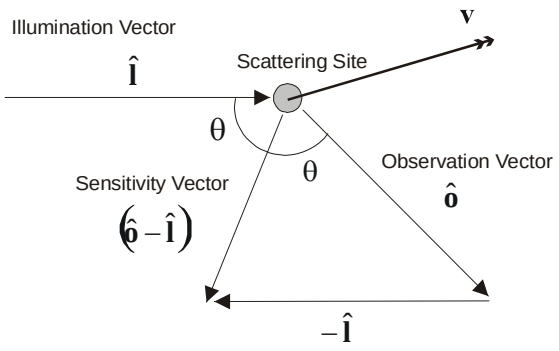

Figure 1 – Doppler Shift Vectors

The result of the observation/illumination vector difference is termed the sensitivity vector, **s**, and components of velocity in this direction give rise to the doppler shift. The components of the vector **s** indicate the sensitivity of the shift to the velocity components u_x, u_y and u_z. For this work a frequency doubled Nd:YAG laser (λ_o=532nm) was used giving a maximum obtainable sensitivity of 3.76MHz per m/s.

Like most optical methods, the flow under investigation requires seeding with particles to enable sufficient scattering of laser light. For sub-sonic flows the particles sizes are chosen primarily on their ability to scatter sufficient light. In the course of this research the seeding was achieved by using a Laskin atomizer with a 50:50 Glycerine/water mixture.

For most aerospace flows the frequency shifts are of the order of 10^7-10^8Hz, which is many orders of magnitude smaller than the incident frequency of 5.6×10^{14}Hz. This prevents resolution of the Doppler shift by absolute frequency measurement.

The key feature of the system described by **Komine and Brosnan (1991)** was the use of an iodine vapour filter to resolve the frequency shift. Iodine exhibits many absorption lines in the tuning range of a Nd:YAG laser The shape of the absorption line is highly dependent on the solid/vapour equilibrium of iodine within the cell. This is controlled by the coldest part of the cell, termed the *Cold Finger*, and a control system developed at Oxford by **Thorpe (1996)** indicated thermal stability to within ±0.003K. By tuning the frequency such that approximately 50% of the laser light is absorbed, any frequency shift due to the motion of particles within the flow cause the amount of light passed through the filter to increase or decrease (see **Fig 2**).

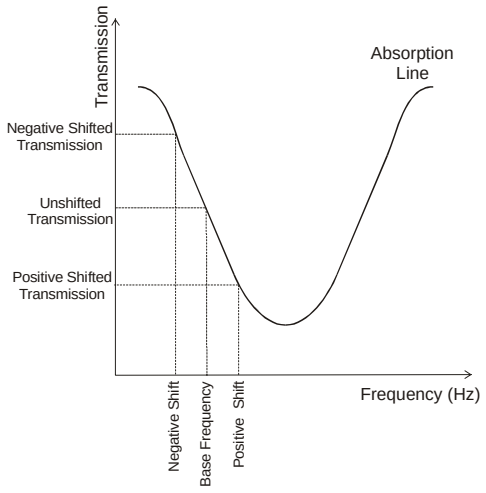

Figure 2 – Resolving The Doppler Shift

By imaging the flow field on a high-resolution CCD camera, proceeded by an iodine absorption filter (of calibrated response), it is possible to determine the frequency shift from the intensity measurement, and through knowledge of the laser/observation geometry, solve for the velocity component. The filtered image of the flow field is termed the *Signal Image*.

There are many other factors which affect the amount of light acquired by the camera, namely variations in laser energy across the sheet, variations in scattering and losses through the optical chain. It is therefore necessary to eliminate these variations by acquiring a second view of the flow field without the iodine filter in place, termed the *Reference Image*. This view can then be used to normalize the filtered image to result in a transmission map dependent only on the shifted frequencies and hence flow velocities.

The **Komine and Brosnan (1991)** system utilized two CCD cameras for the single component measurement, one to acquire the filtered view and

one to acquire the unfiltered normalization view. Work at Oxford University by **Ainsworth *et al* (1997)** enabled a significant simplification of the system by using a array of beam splitting optics and mirrors in order to separate the image into two identical channels and acquire both signal and reference images side by side on a single CCD camera. Schematics of the dual camera and single camera approaches are shown in **Fig 3(a)** and **Fig 3(b)**.

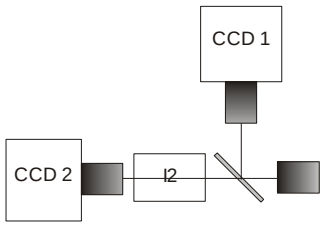

Figure 3(a) – Dual Camera Approach

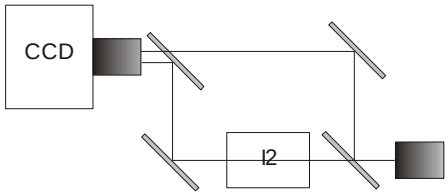

Figure 3(b) – Single Camera Approach

Physical alignment of the Signal and Reference images on the CCD gives poor accuracy and sub-pixel registration is required. Additionally perspective and optical distortions must be removed. This is conducted by taking images of an alignment target (an array of regularly spaced white dots on a black background). The centres of each dots are determined by using an intensity weighting approach and an orthogonal polynomial warping transform is determined to align the two images and remove distortions. Such images are termed *Dewarped*. An extensive discussion of this procedure can be found in **Manners *et al* (1996)**.

3 - MULTI-COMPONENT MEASUREMENT

The majority of previous DGV research has concerned itself with single component measurement. This either arranges the apparatus such that the sensitivity vector is coincident with the u_x velocity component (hence insensitive to u_y and u_z components) or assumes that two of the components are zero (for examples off axis components in a free jet).

For three-component DGV (3C-DGV) the Doppler shift must be resolved for three different sensitivity directions in order to separate the orthogonal velocity components. The sensitivity direction can be changed either by viewing the flow from a fixed position and changing the direction of the laser illumination or viewing from three different directions with a fixed laser direction. The first method is used extensively by **Willert *et al* (2002)** and has the advantages of a simplified imaging system, although repeated experiments are required to resolve each velocity component in turn. This renders this method unsuitable for the three-component measurement of unsteady flow fields. In order to conduct three-component measurement of unsteady flow fields the second method must be used.

In its simplest form simultaneous 3C-DGV consists of three single component DGV systems, which can be either of the dual or single camera type. Although this is perhaps the simplest arrangement in terms of system set up, three temperature stabilised iodine cells are required (and must be calibrated) along with three sets of imaging optics and either three or six high resolution CCD cameras. Additionally the camera exposures must be synchronized. The aim of this research has been the development of a further simplified system to allow simultaneous three-component measurement.

For each point in the flow a frequency shift is determined for each observation direction (f_{D1}, f_{D2} and f_{D3}). Through knowledge of the observation directions and the laser direction the three Doppler shift equations can be arranged in matrix form as,

$$\lambda_o \begin{bmatrix} f_{D1} \\ f_{D2} \\ f_{D3} \end{bmatrix} = \begin{bmatrix} s_{11} & s_{12} & s_{13} \\ s_{21} & s_{22} & s_{23} \\ s_{31} & s_{32} & s_{33} \end{bmatrix} \begin{bmatrix} u_x \\ u_y \\ u_z \end{bmatrix} \quad (3.1)$$

Or in contracted notation as,

$$\lambda_o \mathbf{f} = \mathbf{G}\mathbf{v} \quad (3.2)$$

The **G** matrix coefficients are the corresponding component sensitivities. Once the frequency shifts are known for each point in the flow the orthogonal velocity components are calculated by,

$$\mathbf{v} = \lambda_o \mathbf{G}^{-1}\mathbf{f} \quad (3.3)$$

4 - AMPLIFICATION OF NOISE

Each observation of the frequency shift will contain a certain degree of noise. The combination of the equations to resolve the orthogonal velocity components causes an amplification of the single component noise. The degree of amplification is indicated by the *Condition Number* of the **G**

matrix. The condition number is defined in terms of the matrix N-norm as,

$$\mathrm{cond}(\mathbf{G})_N = \|\mathbf{G}\|_N \left\|\mathbf{G}^{-1}\right\|_N \quad (4.1)$$

Ideally the condition number is equal to unity, which represents the minimum amount of noise amplification owing to the three sensitivity directions being mutually orthogonal. Once the laser direction is defined in the co-ordinate system (usually defined by directions of major flow velocities) the observation directions for unity condition number are constrained in space. For example, the following laser and observation direction set listed produces a **G** matrix, which is a scaled identity matrix,

$$\hat{\mathbf{l}} = \left(\hat{\mathbf{i}} + \hat{\mathbf{j}} + \hat{\mathbf{k}}\right)/\sqrt{3} \quad (4.2)$$

$$\hat{\mathbf{o}}_1 = \left(-\hat{\mathbf{i}} + \hat{\mathbf{j}} + \hat{\mathbf{k}}\right)/\sqrt{3} \quad (4.3)$$

$$\hat{\mathbf{o}}_2 = \left(\hat{\mathbf{i}} - \hat{\mathbf{j}} + \hat{\mathbf{k}}\right)/\sqrt{3} \quad (4.4)$$

$$\hat{\mathbf{o}}_3 = \left(\hat{\mathbf{i}} + \hat{\mathbf{j}} - \hat{\mathbf{k}}\right)/\sqrt{3} \quad (4.5)$$

$$\mathbf{G} = -\frac{2}{\sqrt{3}}\begin{bmatrix} 1 & 0 & 0 \\ 0 & 1 & 0 \\ 0 & 0 & 1 \end{bmatrix} \quad (4.6)$$

Choosing the 2-norm,

$$\mathrm{cond}(\mathbf{G})_2 = 1 \quad (4.7)$$

For any laser direction the observation directions for the unity condition number can be determined by finding the rotational transformation, which transforms the laser vector in the standard case above to the laser vector of interest. This transformation can then be applied to each of the observation vectors to determine the idealized view directions for that geometry. Rotations of this geometry around the laser vector axis are also possible solutions.

This analysis is useful for determining the idealized arrangement for a three-component DGV system and provides a starting point for positioning the observation points, however, it may not yield the measurement with the lowest noise. The noise in each of the single components is highly dependent on the direction of observation (see section 7). Additionally, the idealized vectors may be impractical due to limited optical access on a test rig, may require highly oblique viewing of the laser sheet resulting in poor measurement resolution or may be in a direction of low light scatter.

5 INSTANEOUS MEASUREMENT

The analysis of time-average flow properties can give an insight into the basic behaviour of turbomachinery devices, however, analysis of the time-varying flow structures enables design improvements to be made. Instantaneous DGV makes use of high energy pulsed lasers to illuminate the flow for a very short duration (compared to the fluid dynamic timescale) such that the flow structures are effectively 'frozen' in time. The use of pulsed Nd:YAG lasers for single component velocity measurements in time-varying flows is described by **Thorpe and Ainsworth (1998)** and **Thorpe *et al* (2000)**.

As only a single pulse is used to make the measurement there must be sufficient scattered energy to record a sufficient signal on the CCD camera. Modern CCD cameras may have quantum efficiencies up to 90%, which reduces the amount of incident light required, but the camera performance is still limited by photon statistical shot noise. The Signal to Noise Ratio (SNR) based on shot noise is given by,

$$SNR_{shot} = \sqrt{N_e} \quad (5.1)$$

In order to achieve the best SNR based on shot noise it is necessary to use CCD cameras with large full well capacities. This increases the amount of laser light required to make full use of the dynamic range of the camera.

6 - LASER SYSTEM DESIGN

A custom-made laser system was designed and manufactured for the 3C-DGV research. The key parameters of the system are displayed in **Table 1**. The laser system is a Spectron SL-454G frequency doubled Nd:YAG pulsed laser, which incorporates a Lightwave 101-1064-002 injection seeder specially selected to give 3.5mW output.

Unseeded Nd:YAG lasers have linewidths of ~30GHz (FWHM), which exceeds the width of the iodine absorption features (~2GHz). Passing laser light through an iodine filter is mathematically represented by the convolution of the laser frequency spectrum and the iodine filter response. In order for the absorption to be discernable the laser spectrum must be at least an order of magnitude narrower than the iodine feature. By using an injection seeder the energy held in the lasing medium is extracted by a single cavity mode. The linewidth is almost Fourier limited and is given by equation 6.1 from **Koechner (1999)**,

$$f_L = \frac{2\ln 2}{\pi t_p} \qquad (6.1)$$

Wavelength	532nm
Pulse Duration	~10nS (FWHM)
Pulse Energy	240mJ
Pulse Rate	10Hz
Fourier Limited Linewidth	44MHz
Tuning Range	±20GHz (at 532nm)
Cooling	Water to Water

Table 1 – Summary of Laser Specification

One added complication in DGV is that the frequency of the seeded output needs to be varied to allow calibration of the iodine absorption line. This requires the center frequency of the seed laser to be tuned to the maximum of the gain profile of the host laser so that the output remains seeded as it is tuned away from the centre frequency. The position of the gain profile is set by the temperature of the cooling water and moves by ~2GHz/K. Although this approach produces stable seeding, there is no guarantee that an iodine line will occur near the centre frequency. The Oxford laser system utilizes a control valve on the cooling water circuit, which allows the temperature of the water to be set. This enables the gain profile to be shifted so that the maximum point is aligned closely with an absorption feature. The seeder base frequency can then be tuned to this line to allow stable seeding across the whole tuning range.

Normally the beam energy of pulsed lasers is controlled in one of two ways. Either the voltage to the flash lamps can be modulated to vary the degree of population inversion or the Q-switch opening can be offset from the optimum temporal position. Control of the flash lamp voltage affects the thermal state of the laser, which moves the host gain profile. This can lead to seeding instabilities.

The cavity length is matched to the seeder emission by using a voltage derived from the difference in time between the Q-switch opening and the emergence of the pulse (termed the Build Up Time). Introducing extreme delays in the Q-switch opening time (to reduce the laser energy) affects the ability of the cavity length controller to follow the seeder emission. Additionally, a constant value of the Build Up Time whilst seeded acts as an indication that the laser's output spectrum is stable.

Due to these reasons the laser energy is modulated externally and the laser is treated as a 'black box' illumination source. The modulation is conducted using a half-wave plate, a polarization dependent beam splitter and a beam dump. By rotating the half-wave plate, the relative intensities of the transmitted (sheet forming) and diverted (dumped) beams can be varied continuously. Due to the high energy densities involved (>0.5J/cm^2 in 10nS) it is not possible to use standard beam splitting cubes as the cement layers on the interface have a low energy threshold. Therefore, the beam splitting cube surfaces are held together at the interfaces through highly polished optical contact, which cannot be pulled apart by hand. This cube is optimized for 532nm and has and energy threshold of ~10J/cm^2 in 10nS.

7 - LASER SPECKLE CONSIDERATIONS

One of limiting factors for instantaneous measurement is *Laser Speckle*. The speckle pattern is usually observed when a continuous wave laser strikes a stationary surface. Speckle is due to the interference of out of phase diffraction patterns resulting from roughness elements on the surface. In the case of instantaneous DGV, the flows move very little over the 10nS pulse and therefore a stationary speckle pattern is produced. The speckle holds information about the particle surface and therefore is not technically noise, but due to its deleterious effect on the DGV measurement it is often termed *Speckle Noise*.

Ideally the speckle pattern should be removed by the normalization with the reference channel, however, the pattern is spatially variant and therefore complete removal requires perfect alignment of the signal and reference images and identical optical path lengths. Both of these criteria are in practice impossible to obtain, so the pattern propagates into the final measurement. Experiments conducted at Oxford indicate that large structures in the speckle pattern are partially removed by the reference channel normalization, and additionally the dewarping and interpolation procedures play a role in noise removal. Typically the speckle based SNR in the ratio image is slightly higher than the SNR in each of the signal and reference images.

The random speckle pattern can be partially removed by applying a low pass filtering kernel to each image, although this requires some knowledge *a priori* of likely spatial frequencies involved in the flow field and it is preferable to eliminate the noise as much as possible at source. **Smith (1998)** formed the SNR based on speckle in a single image as,

$$SNR_{speckle} = \frac{\Delta x}{1.2(1+M)F\lambda_o} \qquad (7.1)$$

One of the key parameters in equation 7.1 is the dependence of speckle on the optical F-number. This has been confirmed experimentally by acquiring four images of a stationary disc illuminated for fifty laser pulses. The four images were averaged to reduce the shot noise but to preserve the surface dependent speckle noise. The average image was corrected for stray background light by subtracting an image acquired in the absence of laser light and was normalized using an image averaged over four frames, acquired with the disc rotating to remove the speckle pattern. The normalization frame was also corrected for background light. The SNR was calculated for a region of 53×53 pixels in the reference side of final image. The results are plotted against F-number in **Fig 4** and compared against equation 7.1.

The experimental SNRs are slightly higher than those predicted. This can be explained by the method used to illuminate the disc. The beam profile of a Gaussian laser is highly modulated in the near-field and this is observed when the beam strikes a target directly. This modulation introduces regions of low intensities in the final image, which can cause poor shot noise SNR. This can be improved by placing a polythene disc in the chain of sheet forming optics to partially diffuse the beam. This removes some of the beam coherence and results in less severe interference patterns (higher SNR).

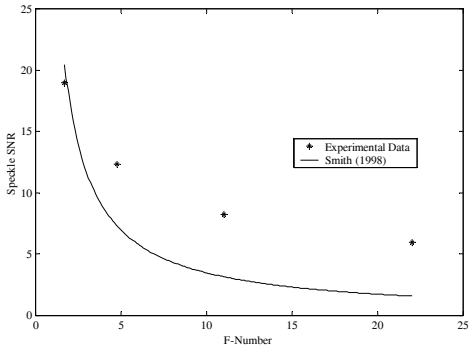

Figure 4 – Dependence of Speckle on F-number

8 - 3C-DGV CCD CAMERA

Examining equation 7.1 enables the parameters affecting speckle to be prioritized for DGV. Typically the magnification, M, is much less than unity and can be neglected. The F-number should be kept low, however, this parameter is coupled with the intensity of the image and the degree of focus and is therefore not freely selectable (see section 10). The wavelength is practically constant across the tuning range and this leaves the pixel dimension, Δx, as the controlling parameter. Equation 7.1 indicates that the pixel dimension should be kept as large as possible to achieve a good SNR. Most commercial CCD cameras have constant chip sizes (typically 25.4mm or 12.7mm) and strive for increased resolution by reducing the pixel dimension. Although high resolution is desirable, an increase in resolution at the expense of pixel dimension will be counteracted by a reduced SNR. In order to improve the SNR on these cameras, pixel binning or extensive low pass filtering is required, which negates the usefulness of increased resolution.

Based on this argument the ideal camera for DGV is a large pixel, high to medium resolution camera. The camera utilized in the course of this research is an Andor Technology 16-bit DW-4K2 25.4mm CCD, with 1024×1024 resolution and 24μm pixels. A full specification for the camera is presented in **Table 2**. The CCD can be electronically cooled to -60°C to limit dark current on long exposures and has a pixel full well capacity of 131070 electrons. This corresponds to a shot noise SNR of 362 prior to saturation (an order of magnitude higher than the speckle SNR).

Model	Andor DW-4K2
Resolution	1024×1024
Pixel Dimension	24μm
A/D Conversion	16 bit
Full Well Capacity	131070 electrons
Quantum Efficiency	55% at 532nm
Cooling	Air to –60°C

Table 2 – Summary of CCD Specification

9 - IMAGING SYSTEM DESIGN

As mentioned in section 3, the simplest three-component imaging system consists of three independent single-component imaging systems. **Nobes *et al* (2002)** demonstrated the use of three imaging fibre bundles to transport the scattering light from three observation directions to a single head unit consisting of a two-camera arrangement. Additionally a fourth bundle branch is used to record the image of the laser light striking a slowly rotating disc. This fourth image allows the determination of the transmission of the unshifted laser frequency. Therefore, four images are acquired on each CCD camera (three view and one frequency reference). This arrangement requires the use of a single temperature stabilized iodine cell.

The new Oxford system utilizes a three-branch set of imaging fibre bundles manufactured by Schott-Fostec. Each branch is 2.78m long and is constructed from 777,600 fibres of 10μm diameter in 7.2mm by 10.8mm format. The fibre centers are arranged on a regular grid. The bundles have a

transmission of approximately 40% at 532nm, this loss is balanced by the increased quantum efficiency of the camera (~55% compared to ~30% with the camera used previously at Oxford).

One end of each branch is collected together in the *Common End Array* which arranges the three rectangular sub-arrays as a combined array of 10.8mm by 22.6mm (3×7.2mm width + 2×0.5mm separation). Imaging from the Common End Array to the camera is conducted on 1:1 magnification, so ~6 fibres map to each pixel. The large pixel approach is primarily based on the reduction of speckle, but it has the added advantage that each pixel has a degree of redundancy in terms of fibre breakage (~0.1% of fibres are broken).

Like the single component system, the three-component system uses only a single camera to capture all the images (see **Fig 6**). These six images (three signal and three reference) are arranged three high and two wide (see **Fig 7**). The bundle aspect ratio is 3:2 in the opposite direction to utilize the whole of the square CCD array. Each view has a maximum resolution of 450×300 pixels which is a slight increase on the 512×256 resolution used in the previous Oxford system (**Ainsworth and Thorpe, 1997**) and at a more usable aspect ratio.

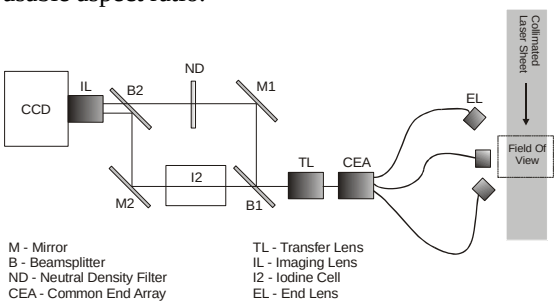

Fig 6 – Schematic of the three-component single CCD camera DGV system

The incident frequency measurement is conducted by a sub-system comprising two integrating photodiodes and a second calibrated iodine cell, which view ~1% of the light split off before the sheet forming optics. The light passes into an integrating sphere to remove speckle before striking a diffuse target, viewed by both photodiodes. The integrating sphere reduces the measurement sensitivity to small variations in beam structure. The photodiode integration is triggered by the laser flash lamp pulse and the signals are recorded on a PC.

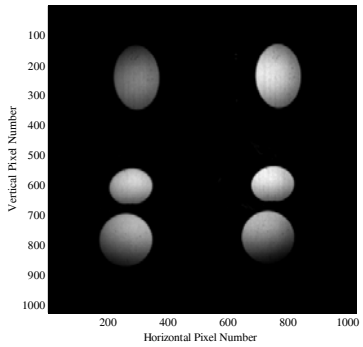

Fig 7 – Three view pairs of a disc captured on a single CCD array

The second iodine cell is constructed under conditions such that only iodine vapour is present. These cells are termed *Starved Cells* and have minimal temperature dependence. This method allows the incident frequency measurement to remain part of the laser system rather than become part of the imaging system. This removes the need for alignment and focusing of a fourth image and frees up valuable CCD resolution for the measurement views.

The two-camera system developed by **Nobes *et al* (2002)** captured four signal images (three measurement and one frequency reference on each camera). Based on the CCD resolution the maximum number of measurements point attainable per component is ~327,000. The Oxford system captures six images (signal and reference) on a single CCD giving a maximum resolution of ~174,000 points per view. However, the Oxford system has pixels which are 3.58 times larger, therefore comparing the systems at similar speckle SNR (by pixel binning) reduces the resolution of the two-camera system by 3.58^2, which gives ~25,500 measurement points per view.

10 - NOVEL IMAGING SYSTEM OPTICS

As light passes through the iodine cell it meets four interfaces corresponding to the two end windows. An empty cell manufactured from Borosilicate Glass has a transmission of approximately 85% due to reflection losses at the interfaces. Some of these reflections are re-reflected back to the camera and form weak 'ghost' images. The light from the ghost images can introduce alignment errors and it is therefore desirable to minimize these reflections. Due to the high temperatures involved during the construction of the cell, it is not possible to use standard anti-reflection coated end windows as the coatings craze under the thermal stresses. Therefore, the iodine cell end windows are coated post-manufacture with a two-layer coating optimized for 532nm. This reduces the ghosting

and increases the throughput of the empty cell to ~92%.

The mirrors and beam splitters are essential parts in the optical system. The primary beam splitter separates the incoming light into signal and reference channels. It is important that the separation occurs at a fixed ratio, without any dependence on polarization. The mirrors are also required to be polarization independent at 45^o incidence. The optical chain of the three-component system handles significantly larger images than in the single component system. In order to reduce light loss the optical chain must be kept as short as possible and large format optics used. Light loss causes attenuation of the images near the edges (vignetting) and although this effect can be removed by normalization, it produces regions of poor SNR. Optics of sufficient size and polarization independence at 532nm could not be sourced commercially. Therefore, the substrates (63mm diameter) had to be coated in-house. The mirrors have a 19-layer coating, whilst the beam splitters are significantly more complicated and are designed in accordance with the method outlined in **Mahlein (1974)** and consist of a 7-layer coating.

In order to minimize the implications of shot noise it is important to fully use the dynamic range of the CCD whilst avoiding saturation. The basis of DGV measurement relies on attenuation of the signal side image. Typically if the reference side image is approaching saturation then the signal side image will be approximately half this intensity, giving a SNR lower by a factor of $\sqrt{2}$. This effect can be removed by placing a neutral density filter with 50% transmission in the reference side. The current system has a mount to hold P-size (85mm square) neutral density filters. Filters with transmissions of 50%, 65% and 80% are used. Coarse matching of the signal and reference intensities, using the filters, allows the full dynamic range to be utilized by increasing the pulse energy.

The alignment and normalization images are acquired by illumination of test cards with broadband laser light. This results in minimal attenuation by the iodine cell and the intensity difference problem is reversed. However, as the normalization and alignment images are stationary frames, the SNR in the low intensity regions can be increased by frame averaging.

The end of each imaging branch is fitted with a cuff with a C-mount thread. An adaptor piece, which screws into the cuff, is used such that standard 35mm format lenses can be used for imaging. The images are formed by the central portion of each lens, which produces high quality images. The enlarged cuffs also allow the ends of the bundles to be held in position with clamps (see **Fig 8**).

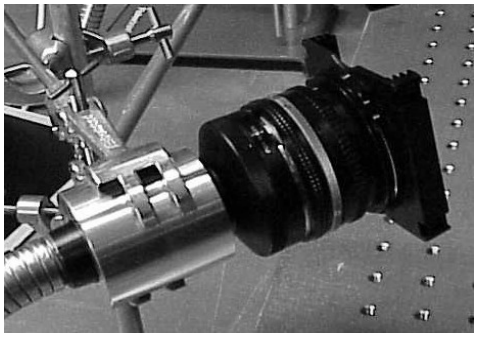

Figure 8 – End Lens with filter holder and clamped bundle cuff

Large mean intensity differences can also occur between each of the three image pairs. The amount of light collected by each end lens is highly dependent on the position due to the shape of the scattering distribution and also the size of the aperture. The intensities of each view can be balanced by control of the aperture sizes for each end lens. However, the depth of field (DOF) of the image is a function of the lens F-number, *F*, where,

$$F = \text{Focal Length} / \text{Aperture Diameter} \qquad (10.1)$$

At high F-numbers the DOF increases as fewer marginal light rays are accepted. For geometries with low condition number, many of the views of the measurement plane will not be orthogonal and thus a reasonable DOF will be required. One option is to control the intensities and focus simultaneously by using high F-numbers, however from equation 7.1 it can be seen that the speckle noise SNR is highly dependent on F-number. Therefore, the F-number must be kept as low as possible, to allow sufficient DOF whilst keeping speckle to a minimum. This coupling effect is broken by using neutral density filters on the end lenses of the system (see **Fig 8**). A-size (65mm square) filters with transmissions of 50%, 65% and 80% can be used to enable coarse equalization of the image intensities. Once the intensities are equalized the full dynamic range can be used by increasing the pulse energy and/or seeding density. The use of neutral density filters provides a simple solution to a complex coupling problem. Once the filters are part of the optical chain, the alignment procedure must be repeated when any are removed, added or moved.

11 - VALIDATION AND FUTURE WORK

The system has been tested by measuring the velocity field of a rotating disc. The raw intensity

camera frame can be seen in **Fig 7**. Despite being a simple velocity field the disc is an unsatisfactory test for 3C-DGV for two reasons. Firstly spatial variations of velocity are linear (low frequency) and therefore acceptable instantaneous results can be achieved by heavy low pass filtering of the images. Secondly all three of the observation points are generally located on the same side of the disc resulting in a poorly conditioned system.

The preliminary system tests indicated that the transmission maps for each component were consistent with those expected for the disc velocity distribution. These tests were carried out with non-polarizing beam splitters optimized for an Argon Ion laser (514.5nm), and therefore an additional randomized noise field would be present when using 532nm laser light. The vignetting of the image at the edges is due to the losses when collimating the light from the fibre bundle output and losses through the system. The enlarged beam splitters and mirrors, described in section 10, will help to alleviate this problem and a new 60mm diameter iodine cell is currently being constructed.

The first full system tests will be carried out on a rotating disc to show the importance of the condition number, and then an investigation of free jet flow and swirled jet flow will be conducted. Additionally, a new short-duration facility for examining the flow over a turbine blade tip has been developed. This facility has good optical access and the flow can also be seeded. The pressure ratio can be varied by a downstream valve and representative Mach and Reynolds numbers exist for 2-4 seconds. The facility allows various tip geometries to be tested and arrays of pressure tappings on the tip allow for comparison of the pressure and velocity fields with CFD.

12 - CONCLUSIONS

A three-component DGV system has been designed and constructed. The system is optimized for instantaneous measurement but is also capable of acquiring time-average measurements. The novel feature of this system is that only a single CCD camera is required to make a simultaneous three-component instantaneous measurement. Unlike most DGV work, this research utilizes a large pixel camera to reduce speckle noise at source such that minimal low pass filtering of the speckle noise is required.

The use of neutral density filters on the end lenses allows the full dynamic range of the camera to be used without adjusting the lens apertures (increasing speckle).

Application of an anti-reflection coating to the iodine cell windows post-manufacture has increased the basic throughput of the cell and reduced errors caused by image ghosting.

The system has undergone successful initial validation and is now being used to measure flows relevant to turbomachinery. Continuing CCD camera and laser development will allow 3C-DGV to progress towards acquisition rates used in PIV.

One of the most attractive features of DGV is the increased resolution of measurements over PIV. Additionally, the single pulse nature of the technique gives improved temporal resolution. For instantaneous DGV speckle is the dominant cause of uncertainty. This uncertainty can be reduced either by sacrificing spatial resolution (filtering/binning) or temporal resolution (longer pulses).

ACKNOWLEDGMENTS

The authors would like to acknowledge the support of Isis Innovation Ltd, the laser advice from Dr S. Keen at GSI Lumonics and Mr C. Goodwin at the Department of Physics of Oxford University.

REFERENCES

Ainsworth, R.W., Thorpe, S.J., and Manners, R.J., 1997, *A New Approach to Flow-Field Measurement - a View of Doppler Global Velocimetry Techniques*, Int. J. Heat and Fluid Flow, Vol.18, pp. 116-130.

Koechner W., 1999, *Solid State Laser Engineering*, 5th Edition, Springer-Verlag (Berlin Heidelberg), ISBN-3-540-65064-4.

Komine H., and Brosnan S.J., 1991, *Instantaneous, Three-Component Doppler Global Velocimetry*, Laser Anemometry, Vol 1, pp. 273-277, ASME.

Lawson N.J, 2004, *The application of laser measurement techniques to aerospace flows*, Proceedings of IMechE, Vol. 218, Part G, J. Aerospace Engineering.

Mahlein H.F., 1979, *Non-Polarizing Beam Splitters*, Optic Acta, Vol. 21, No. 7, pp. 577-583.

Manners R.J., Thorpe S.J., and Ainsworth R.W., 1996, *Image Processing Techniques for Doppler Global Velocimetry*. Proceedings of Optical Methods and Data Processing in Heat and Fluid Flow, City University, London, Great Britain.

Nobes D., Ford H., and Tatam R., 2002, *Three Component Planar Doppler Velocimetry Using Imaging Fibre Bundles*, Proceedings of the 11th International Symposium on Applications of Laser Techniques to Fluid Mechanics, 8th-11th July 2002 Lisbon, Portugal.

Smith M.W., 1998, *The reduction of laser speckle noise in Planar Doppler Velocimetry systems*, NASA Langley Research Council, Hampton, Virginia, AIAA Paper 98-2607.

Thorpe, S.J., 1996, *A Study of Doppler Global Velocimetry in its Application to Aerodynamic Flows*, DPhil Thesis, University of Oxford.

Thorpe, S.J., and Ainsworth, R.W., 1998, *Some consequences of the use of a pulsed Neodymium YAG Laser as illumination source for Doppler Global Velocimetry Measurements*, Proc of 14th Symposium on Measuring Techniques in Transonic and Supersonic flow in Cascades and Turbomachines, Limerick.

Thorpe, S.J., Quinlan, N., and Ainsworth, R.W., 2000, *The Characterisation and Application of a Pulsed Neodymium YAG Laser DGV System to a Time-Varying High-Speed Flow*, Journal of Optics and Laser Technology, Vol 32, Issue 7-8, pp. 543-555, ISSN 0030-3992.

Willert C., Röhle I., Schodl R., Dingle O., and Seidel T., 2002, *Application of Planar Doppler Velocimetry within Piston Engine Cylinders*, Proceedings of the 11th International Symposium on Applications of Laser Techniques to Fluid Mechanics, 8th-11th July 2002 Lisbon, Portugal.